Journal of Complex Networks, 2025, **00**, cnaf013
https://doi.org/10.1093/comnet/cnaf013
Advance access publication 00 Month 2025
Article

OXFORD

Vertex-wise graph's spectral density decomposition and its applications

Grover E.C. Guzman[1], Daniel Yasumasa Takahashi[2], and André Fujita [3,4,*]

[1]Department of Computer Science, Institute of Mathematics and Statistics, University of São Paulo, Rua do Matão, 1010, São Paulo, SP 05508-090, Brazil;
[2]Brain Institute, Federal University of Rio Grande do Norte, Av. Senador Salgado Filho, 3000 Natal, RN 59078-970, Brazil;
[3]Department of Computer Science, Institute of Mathematics and Statistics, University of São Paulo, Rua do Matão, 1010, São Paulo, SP 05508-090, Brazil
[4]Division of Network AI Statistics, Medical Institute of Bioregulation, Kyushu University, Westwing Building 8F 801, Hospital Campus Maidashi 3-1-1, Higashi-ku, Fukuoka, Fukuoka, 812-8582, Japan

*Corresponding author. andrefujita@usp.br. Division of Network AI Statistics, Medical Institute of Bioregulation, Kyushu University, Westwing Building 8F 801, Hospital Campus Maidashi 3-1-1, Higashi-ku, Fukuoka, Fukuoka, 812-8582, Japan.

ABSTRACT

The spectral density of a graph is a key concept for quantitatively characterizing empirical networks. It has many applications, including community detection, graph signal processing, spectral embedding, network evolution, brain network analysis, and random graph modeling. The graph's spectral density is also crucial in developing statistical methods for graphs, such as model selection and comparative testing. Despite its broad applicability, a complete understanding of the relationship between a graph's spectral density and structure remains elusive. To advance our understanding of the relationship between graph spectra and their structure, we introduce a vertex-wise decomposition of the graph's spectral density, allowing us to determine each vertex's contribution to specific eigenvalues. We show that the decomposition of distinct isospectral graphs (graphs with identical spectra) can be distinguished by the vertex-wise graph spectra, showing that the proposed new quantities are finer invariants between isomorphic graphs. Finally, we apply these insights to analyze chemical molecules and identify genes associated with normal versus tumoral breast gene interaction networks.

KEYWORDS: Spectral distribution; vertex decomposition; random graphs; localization.
2000 Math Subject Classification: 15A18, 15B57, 05C82.

1. INTRODUCTION

A graph's spectral density refers to the distribution of eigenvalues of a graph's adjacency matrix (or Laplacian matrix). It represents the frequency or density of eigenvalues.

Graph spectral density has various applications across different fields due to its ability to capture structural properties and connectivity patterns in complex networks. Some of the critical applications of a graph's spectral density include community detection [1, 2], graph signal processing [3], spectral embedding [4, 5], network evolution and growth [6–8], brain network analysis [8–10], and random graph models [11–13].

Received: 12 February 2025. **Editorial decision:** 29 April 2025. **Accepted:** 2 June 2025

More recently, spectral density has also proved critical in developing graph statistical tools [14]. Takahashi *et al.* [14] introduced a general statistical framework based on the graphs' spectral density. They proposed a parameter estimator similar to the maximum likelihood estimator [14, 15], a model selection approach similar to the Akaike Information Criterion [13, 14], and a comparison test similar to the t-test for graphs using the spectral density associated with the graph's adjacency matrix. Later, De Domenico and Biamonte [16] published a parameter estimator and model selection approach using a similar idea based on the spectral density of the graph's Laplacian matrix. Then, many other statistical tools have been proposed: a comparison test for two or more (sets of) graphs like ANOVA [10, 17], a concept of correlation between vectors of graphs [18], Granger causality between time series of graphs [19], and supervised [20] and unsupervised [2] classification approaches.

Although spectral density is an exciting framework for constructing statistical tools for graphs, this approach has a bottleneck: It lacks interpretation. Suppose a spectral density-based statistical test like analysis of graph variability (ANOGVA) [17] suggests that two graphs present different spectral densities. Then, the next question is: Which vertices are differentially connected, or which graph structures are different? To answer these questions, we should identify the regions where the spectral densities differ the most (i.e. the eigenvalues with the most differential frequency). Then, based on those eigenvalues, identify the related structures. However, identifying the relationship between the eigenvalue and the graph's structure is not trivial [21]. Dorogovtsev *et al.* [22] were the first to identify some structures that give rise to eigenvalue 0 in locally tree-like graphs. Golinelli [23] identified some structures that generate eigenvalues 0, ± 1, and $\pm\sqrt{2}$ in large random trees. Kamp and Christensen [24] studied the association of graph motifs with eigenvalues 0 and 2 in the *Drosophila melanogaster*'s protein–protein interaction network. Yadav and Jalan [25] identified three structures that generate the eigenvalue 0 and their biological origins. Marrec and Jalan [26] identified two structures that generate the eigenvalue -1. They also proposed an algorithm to identify them. However, their method only identifies a few patterns [25, 26].

Here, we aim to understand better the relationship between the graph's spectral density and structure. To this end, we present a vertex-wise graph's spectral density decomposition and its relationship with eigenvector localization. Based on this, we calculate the contribution of each vertex to the spectral density—that is, how much each vertex contributes to the appearance of a specific eigenvalue. Finally, we associate the vertex-wise graph's spectral density with the number of closed walks to that vertex.

2. GRAPH'S SPECTRAL DENSITY

Let $G = (V, E)$ be an undirected graph composed of a set V of n vertices and a set E of edges. Let $\mathbf{A}$ be its $n \times n$ symmetric adjacency matrix. We call the set of eigenvalues $\lambda_1 \geq \lambda_2 \geq \ldots \geq \lambda_n$ and their respective eigenvectors $\{\mathbf{v}_1, \mathbf{v}_2, \ldots, \mathbf{v}_n\}$ of $\mathbf{A}$ as the spectrum of G. Let δ be the Dirac delta function. Then we can define the spectral density $\rho(\lambda)$ as follows:

$$\rho(\lambda) = \frac{1}{n} \sum_{i=1}^{n} \delta(\lambda - \lambda_i). \tag{2.1}$$

Based on the arguments of [27–29], we can rewrite Equation (2.1) as follows. First, we express the Dirac delta function of Equation 2.1) as the limit of a Cauchy distribution

$$\delta(\lambda) = -\frac{1}{\pi} \lim_{\varepsilon \to 0^+} \mathrm{Im} \frac{1}{\lambda + \mathrm{i}\varepsilon}. \tag{2.2}$$

Then, substituting Equation (2.2) into Equation (2.1), we have that

$$\rho(\lambda) = \lim_{\varepsilon \to 0^+} -\frac{1}{n\pi} \mathrm{Im} \sum_{i=1}^{n} \frac{1}{\lambda - \lambda_i + \mathrm{i}\varepsilon}. \tag{2.3}$$

Set $z = \lambda + \mathrm{i}\varepsilon$ and define the smoothed spectral density

$$\begin{aligned} \rho_\varepsilon(\lambda) &= -\tfrac{1}{n\pi} \mathrm{Im} \sum_{i=1}^{n} \tfrac{1}{z-\lambda_i}, \\ &= -\tfrac{1}{n\pi} \mathrm{Im} \left(\mathrm{tr}(z\mathbf{I} - \mathbf{A})^{-1} \right). \end{aligned} \tag{2.4}$$

In the last equality of Equation (2.4), we used the fact that, for a nonsingular diagonalizable $n \times n$ matrix $\mathbf{M}$ with eigenvalues $\beta_1, \beta_2, \ldots, \beta_n$, the trace of $\mathbf{M}^{-1}$ is the sum of $\beta_1^{-1}, \beta_2^{-1}, \ldots, \beta_n^{-1}$. The parameter ε determines the smoothness of the smoothed spectral density $\rho_\varepsilon(\lambda)$ [27] and

$$\rho_\varepsilon(\lambda) \xrightarrow[\varepsilon \to 0^+]{} \rho(\lambda).$$

Equation (2.4) was first derived in the Quantum Chaos community [30] to calculate the density of states of a quantum mechanical system. Besides, [31] expressed the spectral density using the eigenvectors $\mathbf{V} = [\mathbf{v}_1, \mathbf{v}_2, \ldots, \mathbf{v}_n]$ of $\mathbf{A}$ as follows:

$$\begin{aligned} \rho_\varepsilon(\lambda) &= -\tfrac{1}{n\pi} \mathrm{Im}(\mathrm{tr}(z\mathbf{I} - \mathbf{A})^{-1}), \\ &= -\tfrac{1}{n\pi} \mathrm{Im} \left\{ \mathrm{tr} \left(\mathbf{V} \mathrm{diag}(\tfrac{1}{z-\lambda_1}, \tfrac{1}{z-\lambda_2}, \ldots, \tfrac{1}{z-\lambda_n}) \mathbf{V}^\top \right) \right\}, \\ &= -\tfrac{1}{n\pi} \mathrm{Im} \left\{ \mathrm{tr} \left(\sum_{i=1}^{n} \tfrac{1}{z-\lambda_i} \mathbf{v}_i \mathbf{v}_i^\top \right) \right\}, \\ &= -\tfrac{1}{n\pi} \sum_{i=1}^{n} \mathrm{tr}(\mathbf{v}_i \mathbf{v}_i^\top) \mathrm{Im}(\tfrac{1}{z-\lambda_i}), \\ &= \tfrac{1}{n} \sum_{i=1}^{n} \sum_{j=1}^{n} |\mathbf{v}_{j,i}|^2 \mathrm{Im}(-\tfrac{1}{\pi} \tfrac{1}{z-\lambda_j}), \\ &\xrightarrow[\varepsilon \to 0^+]{} \tfrac{1}{n} \sum_{i=1}^{n} \sum_{j=1}^{n} |\mathbf{v}_{j,i}|^2 \delta(\lambda - \lambda_j), \end{aligned} \tag{2.5}$$

where $v_{j,i}$ is the (j, i)th element of $\mathbf{V}$.

Another way of expressing Equation (2.4) is by using the number of closed walks w_i^l of length l from vertex i [32]:

$$\begin{aligned} \rho_\varepsilon(\lambda) &= -\tfrac{1}{n\pi} \mathrm{Im}(\mathrm{tr}(z\mathbf{I} - \mathbf{A})^{-1}), \\ &= -\tfrac{1}{n\pi} \mathrm{Im}(\tfrac{1}{z} \sum_{l=0}^{\infty} \tfrac{\mathrm{tr}(\mathbf{A}^l)}{z^l}), \\ &= -\tfrac{1}{n\pi} \mathrm{Im}(\tfrac{1}{z} \sum_{i=1}^{n} \sum_{l=0}^{\infty} \tfrac{\mathbf{A}_{i,i}^l}{z^l}), \\ &= -\tfrac{1}{n\pi} \mathrm{Im}(\tfrac{1}{z} \sum_{i=1}^{n} \sum_{l=0}^{\infty} \tfrac{w_i^l}{z^l}). \end{aligned} \tag{2.6}$$

Equation (2.6) shows that the spectral density is related to the number of closed walks of any length on the graph. If two vertices have the same number of closed walks of any length, their spectral density functions will be the same, but the converse might not be true. The relationship between spectral density and closed walks is already known [33].

3. VERTEX-WISE GRAPH'S SPECTRAL DENSITY DECOMPOSITION

In this section, we obtain the vertex-wise graph's spectral density decomposition.

Notice that we can rewrite Equation (2.6) as follows:

$$\begin{aligned}\rho_{\varepsilon}(\lambda) &= -\tfrac{1}{n\pi}\mathrm{Im}(\tfrac{1}{z}\sum_{i=1}^{n}\sum_{l=0}^{\infty}\tfrac{w_i^l}{z^l}),\\ &= -\tfrac{1}{n\pi}\mathrm{Im}(\tfrac{1}{z}\sum_{i=1}^{n}\sum_{l=0}^{\infty}\tfrac{\mathbf{A}_{i,i}^l}{z^l}),\\ &= -\tfrac{1}{n\pi}\sum_{i=1}^{n}\mathrm{Im}((z\mathbf{I}-\mathbf{A})_{i,i}^{-1}).\end{aligned} \tag{3.1}$$

In Equation (3.1), we can observe that, the ith diagonal element of $(z\mathbf{I}-\mathbf{A})^{-1}$ is a weighted sum of the closed walks of vertex i. With this in mind, we can express that the spectral density of the graph is the mean of the diagonal elements $\rho_{i,\varepsilon}(\lambda), \forall i = 1,\ldots,n$, given by:

$$\begin{aligned}\rho_{i,\varepsilon}(\lambda) &= -\tfrac{1}{\pi}\mathrm{Im}((z\mathbf{I}-\mathbf{A})_{i,i}^{-1}),\\ &= -\tfrac{1}{\pi}\mathrm{Im}(\tfrac{1}{z}\sum_{l=0}^{\infty}\tfrac{w_i^l}{z^l}).\end{aligned} \tag{3.2}$$

This observation naturally suggests the following definition for the spectral density associated with the ith vertex.

$$\rho_i(\lambda) = \lim_{\varepsilon\to 0^+} -\frac{1}{\pi}\mathrm{Im}((z\mathbf{I}-\mathbf{A})_{i,i}^{-1}). \tag{3.3}$$

Also, by considering Equation (2.5), we can express $\rho_i(\lambda)$ in terms of the eigenvalues and eigenvectors of $\mathbf{A}$ as follows. Let $\mathbf{v}_{j,i}$ be the i-th element of the jth eigenvector. Then,

$$\begin{aligned}\rho_i(\lambda) &= \sum_{j=1}^{n}|\mathbf{v}_{j,i}|^2[-\tfrac{1}{\pi}\lim_{\varepsilon\to 0^+}\mathrm{Im}(\tfrac{1}{z-\lambda_j})],\\ &= \sum_{j=1}^{n}|\mathbf{v}_{j,i}|^2\delta(\lambda-\lambda_j).\end{aligned} \tag{3.4}$$

Considering Equations (3.3) and (3.4), we observe that two isospectral graphs (with the same set of eigenvalues, i.e. the same spectral densities) [32] may have different vertex-wise graph spectral densities. However, by construction, all graphs with the same vertex-wise spectral density are isospectral. In practice, to approximate the vertex-wise spectral density, we will use the smoothed version with small ε and a discretization of the interval $[\lambda_n, \lambda_1]$. See Fig. 1 for an example using $\varepsilon = 0.01$.

From Equation (3.4), we can deduce that the importance of ith vertex for an eigenvalue λ is proportional to the weighted sum of the square of the entries of the ith element of all eigenvectors. Hence, when $\varepsilon \to 0^+$, the ith vertex's importance will be the eigenvector's squared ith entry corresponding to the eigenvalue λ. All vertices will have the same importance when the eigenvector is delocalized (all its entries are equal); otherwise, when the eigenvector is localized, a subset of the vertices will have more importance than the others [34]. Jalan et al. [26, 35, 36] used the localization of the eigenvectors to identify some structures related to eigenvalue -1. Dorogovtsev et al., Yadav and Jalan, and Rai et al. [22, 25, 36] propose to use the entries of the eigenvectors associated with 1 and 0 to identify some structures that generate such eigenvalues. The largest eigenvalue is related to the largest degree in the graph [37], and we could also look at the entries of its corresponding eigenvector to identify the vertices that generate the largest eigenvalue.

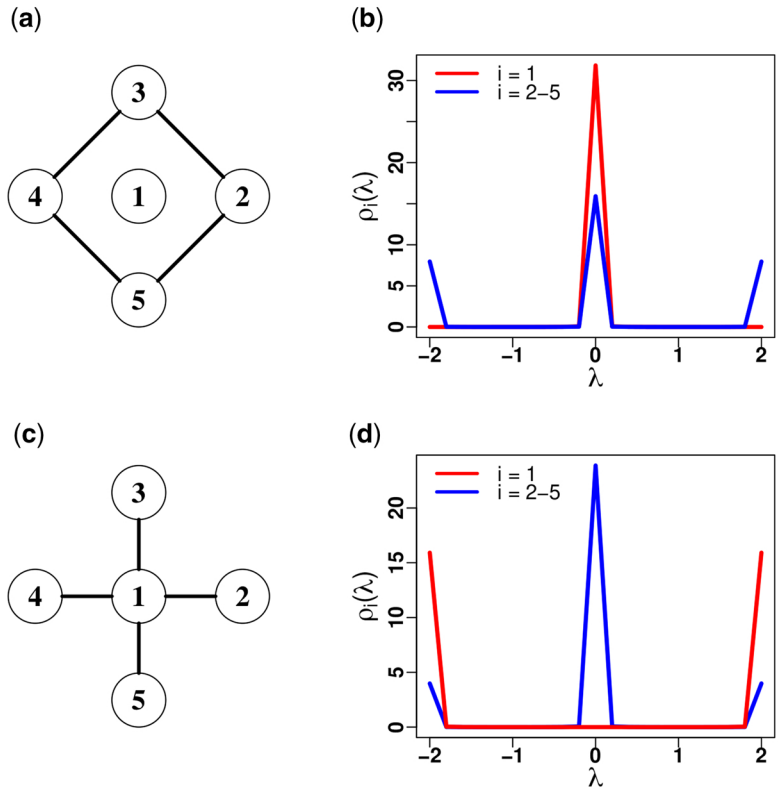

Figure 1. Vertex-wise graph's spectral density decomposition for two isospectral graphs. Panels (a) and (c) illustrate two isospectral graphs. Both graphs have the same set of eigenvalues, i.e. $-2, 0, 0, 0, 2$. Panels (b) and (d) show the spectral decompositions of the graphs described in panels (a) and (c), respectively. The red line represents the spectral density of vertex 1. In contrast, the blue line represents the spectral density of vertices 2, 3, 4, and 5. To obtain the vertex-wise decomposition, we used Equation (3.3) with $\varepsilon = 0.01$, and discretized the interval $[-2, 2]$ in 40 points.
Alt text: Side-by-side comparison of two isospectral graphs and their vertex-wise spectral density decompositions. Panels (a) and (c) display different graph structures that share the same set of eigenvalues {–2, 0, 0, 0, 2}. Panels (b) and (d) show the corresponding vertex-wise spectral density plots. Red lines represent the spectral density of vertex 1, while blue lines represent vertices 2–5. These visualizations demonstrate that although the graphs have identical spectra, their vertex-level contributions differ.

We generated graphs using the Watts-Strogatz [38] and Barabási-Albert [33] models with different parameters to show how our proposed method works. Then, we computed the contribution of their vertices to the eigenvalues -1, 1, 0, and λ_1 (largest eigenvalue).

Figure 2 shows the contribution of the vertices for a graph generated using the Watts-Strogatz model with 40 vertices, a mean degree of $\bar{d} = 4$, and a rewiring probability p_w of zero. This configuration generates a regular ring lattice graph vertex-transitive [39]. Panel (a) depicts the graph to be analyzed. Panel (b) describes the associated spectral density. Panels (c) and (d) highlight the vertices associated with $\lambda = -1$ and $\lambda = 1$. Panel (e) shows the vertices associated with $\lambda = 0$. Panel (f) shows the vertices associated with the largest eigenvalue. We can observe that for all eigenvalues, the contribution of the vertices to the considered eigenvalue is the same. This happens because vertex-transitive graph eigenvectors are delocalized [40]. Hence, the contribution of the vertices will be the same for any eigenvalue.

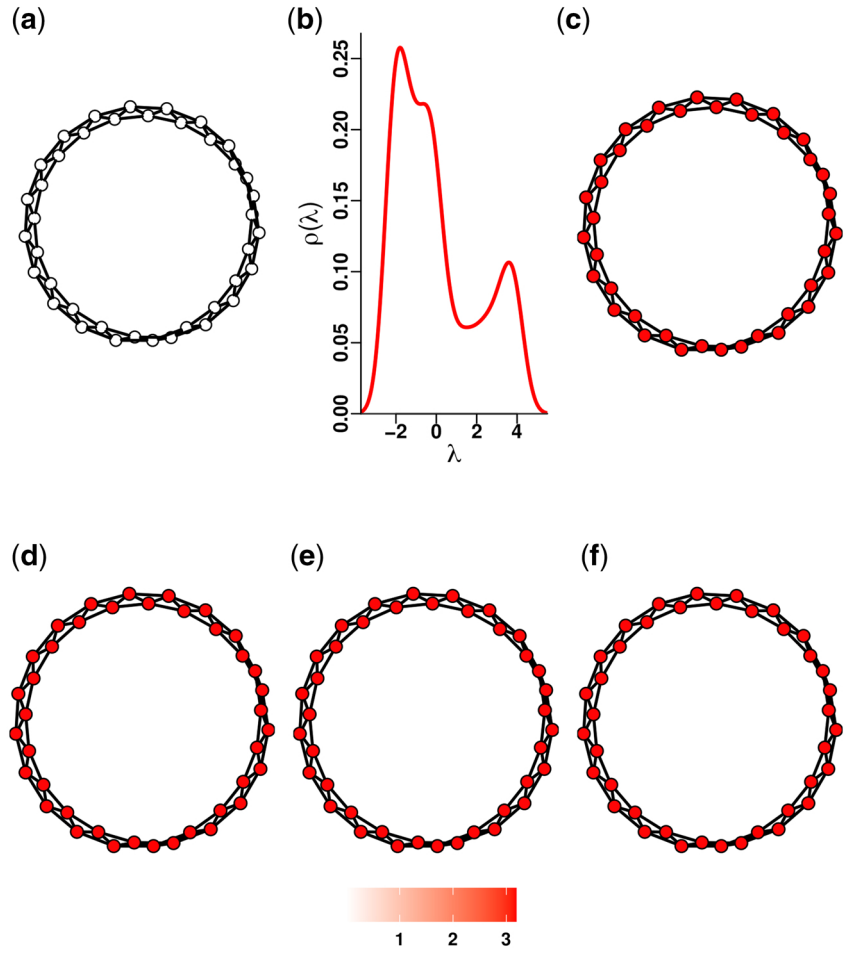

Figure 2. The darker red the vertex is, the higher its contribution to the considered eigenvalue. (a) Example of a graph generated with the Watts-Strogatz model with a rewiring probability $p_w = 0.0$ and mean degree $\bar{d} = 4$. (b) The spectral density of the graph described in panel (a). (c) Vertices related to the eigenvalue –1 ($\rho_i(\lambda = -1)$). (d) Vertices related to the eigenvalue +1 ($\rho_i(\lambda = +1)$). (e) Vertices related to the eigenvalue 0 ($\rho_i(\lambda = 0)$). (f) Vertices related to the largest eigenvalue ($\rho_i(\lambda = \lambda_1)$). To obtain the contribution of each vertex to a particular eigenvalue, we used Equation (3.3) with $\varepsilon = 0.01$.
Alt text: Visualization of vertex contributions to specific eigenvalues in a Watts-Strogatz graph. Panel (a) shows a network generated with a rewiring probability pw = 0.0 and average degree d = 4. Panel (b) displays the graph's spectral density. Panels (c-f) highlight vertex-wise contributions to individual eigenvalues: –1, +1, 0, and the largest eigenvalue ($\lambda 1$), respectively. Vertex color intensity (red) indicates the magnitude of contribution—darker red means a higher contribution.

Figure 3 shows the contribution of the vertices for a graph generated using the Watts-Strogatz model with 40 vertices, a mean degree $\bar{d} = 4$, and a rewiring probability p_w of 0.10. Unlike the previous example, we broke the symmetry of the ring lattice structure. Hence, some vertices make more contributions than others.

Figure 4 shows the contribution of the vertices for a graph generated using the Barabási-Albert [33] model with 40 vertices, a mean degree $m = 2$, and a scaling parameter $\gamma = 0.5$. We can observe that only a subset of vertices contribute to the presence of an eigenvalue, which means there exists a localization in the eigenvectors near the considered eigenvalues. In particular, for the largest

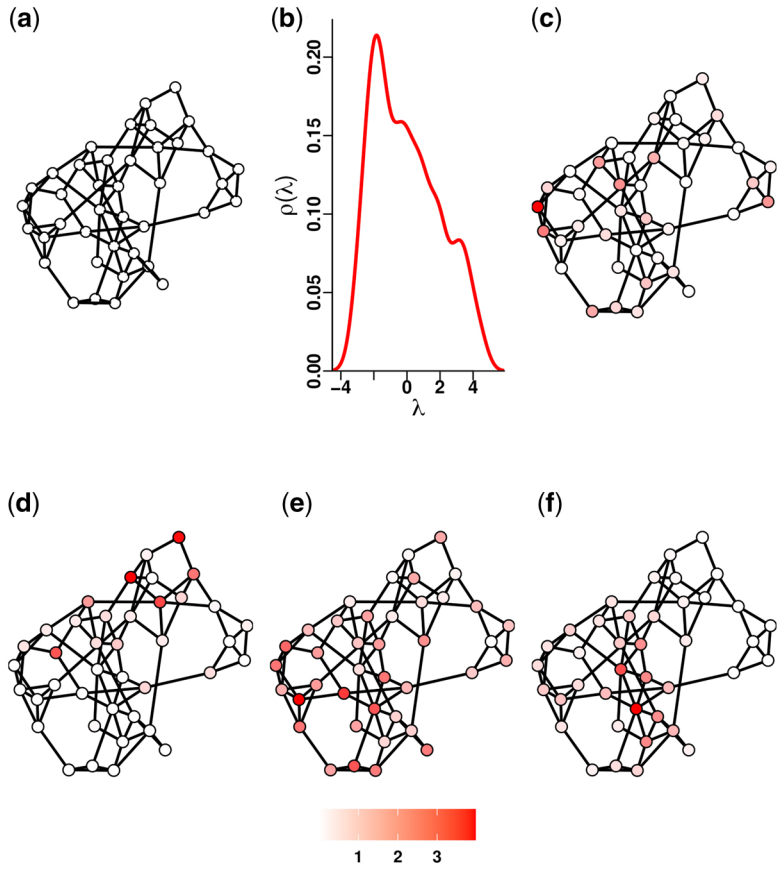

Figure 3. The darker red the vertex is, the higher its contribution to the considered eigenvalue. (a) Example of a graph generated with the Watts-Strogatz model with a rewiring probability $p_w = 0.10$ and mean degree $\bar{d} = 4$. (b) The spectral density of the graph described in panel (a). (c) Vertices related to the eigenvalue –1 ($\rho_i(\lambda = -1)$). (d) Vertices related to the eigenvalue +1 ($\rho_i(\lambda = +1)$). (e) Vertices related to the eigenvalue 0 ($\rho_i(\lambda = 0)$). (f) Vertices related to the largest eigenvalue ($\rho_i(\lambda = \lambda_1)$). To obtain the contribution of each vertex to a particular eigenvalue, we used Equation (3.3) with $\varepsilon = 0.01$.
Alt text: Visualization of vertex contributions to specific eigenvalues in a Watts-Strogatz graph. Panel (a) shows a network generated with a rewiring probability pw = 0.0. and average degree d=4. Panel (b) displays the graph's spectral density. Panels (c-f) highlight vertex-wise contributions to individual eigenvalues: –1, +1, 0, and the largest eigenvalue ($\lambda 1$), respectively. Vertex color intensity (red) indicates the magnitude of contribution—darker red means a higher contribution.

eigenvalue, we can observe that the vertices with the largest contribution are the ones with the largest degree and the nearby vertices. This phenomenon of localization of the largest eigenvalue was found in [34] and happens when the scaling parameter is smaller than 5/2.

Figure 5 shows the contribution of the vertices for a graph generated using the Barabási-Albert [33] model with 40 vertices, a mean degree $m = 2$, and a scaling parameter $\gamma = 3.0$. Since the scaling factor is large, many peripheral vertices connect to the same (hub) vertices. Thus, those peripheral vertices contribute to the presence of eigenvalue 0 [25, 26, 35, 36]. Also, for the largest eigenvalue, we can observe that the vertices with the largest contribution are the ones with the largest degree. Pastor-Satorras and Castellano [34] found this phenomenon of localization of the largest eigenvalue. It happens when the scaling parameter is greater than 5/2.

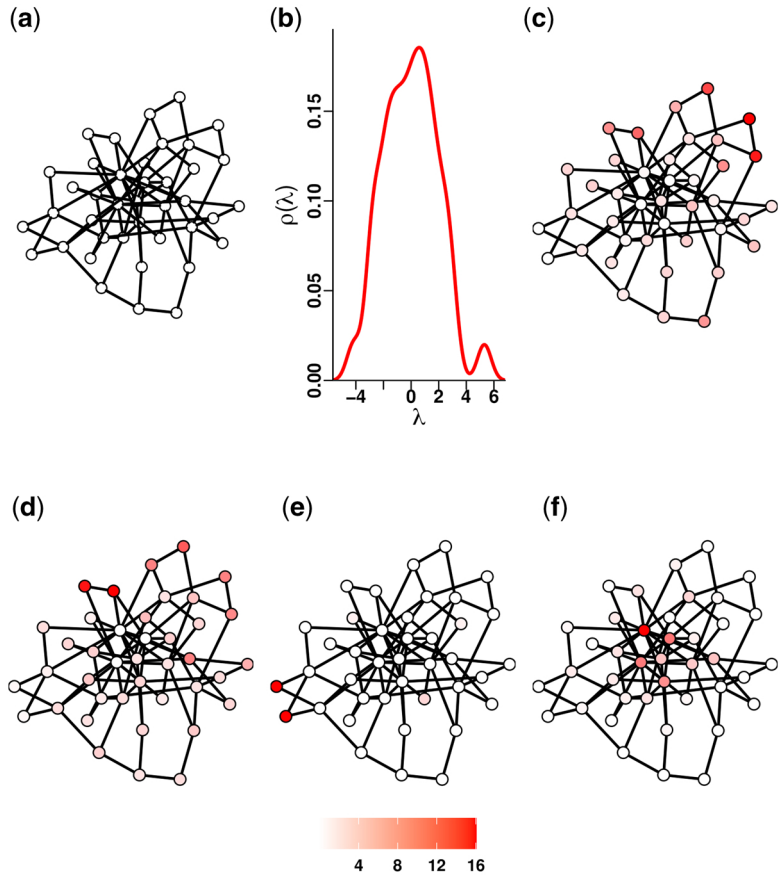

Figure 4. The darker red the vertex is, the higher its contribution to the considered eigenvalue. (a) Example of a graph generated with the Barabási-Albert model with a scaling parameter $\gamma = 0.5$ and mean degree $m = 2$. (b) The spectral density of the graph described in panel (a). (c) Vertices related to the eigenvalue –1 ($\rho_i(\lambda = -1)$). (d) Vertices related to the eigenvalue +1 ($\rho_i(\lambda = +1)$). (e) Vertices related to the eigenvalue 0 ($\rho_i(\lambda = 0)$). (f) Vertices related to the largest eigenvalue ($\rho_i(\lambda = \lambda_1)$). To obtain the contribution of each vertex to a particular eigenvalue, we used Equation (3.3) with $\varepsilon = 0.01$.
Alt text: Visualization of vertex contributions to specific eigenvalues in a Barabási-Albert graph with scaling parameter $\gamma = 05$ and mean degree m = 2. Panel (a) displays the graph structure. Panel (b) shows the graph's spectral density. Panels (c)-(f) highlight vertex-wise contributions to the eigenvalues –1, +1, 0, and the largest eigenvalue ($\lambda 1$), respectively. Vertex color intensity (darker red) represents a higher contribution of that vertex to the corresponding eigenvalue.

Figure 6 shows the contribution of the vertices for a graph generated using the Erdős-Rényi [41] model with 40 vertices. We set the probability p of adding an edge between two vertices as 0.103. The reason is to produce graphs with an average degree of 4, i.e. the same as the graph generated using the Watts-Strogatz model. The graph generated using the Erdös-Rényi model, with 40 vertices and $p = 0.103$, does not exhibit significant symmetric structures. Therefore, only a pair of vertices contributes to the presence of the eigenvalues $\lambda = \pm 1$. Additionally, only three vertices contribute to the presence of the eigenvalue $\lambda = 0$, two of which are leaf vertices, and one is an isolated vertex. Due to the lack of symmetry, some vertices contribute more than others to the largest eigenvalue (λ_1).

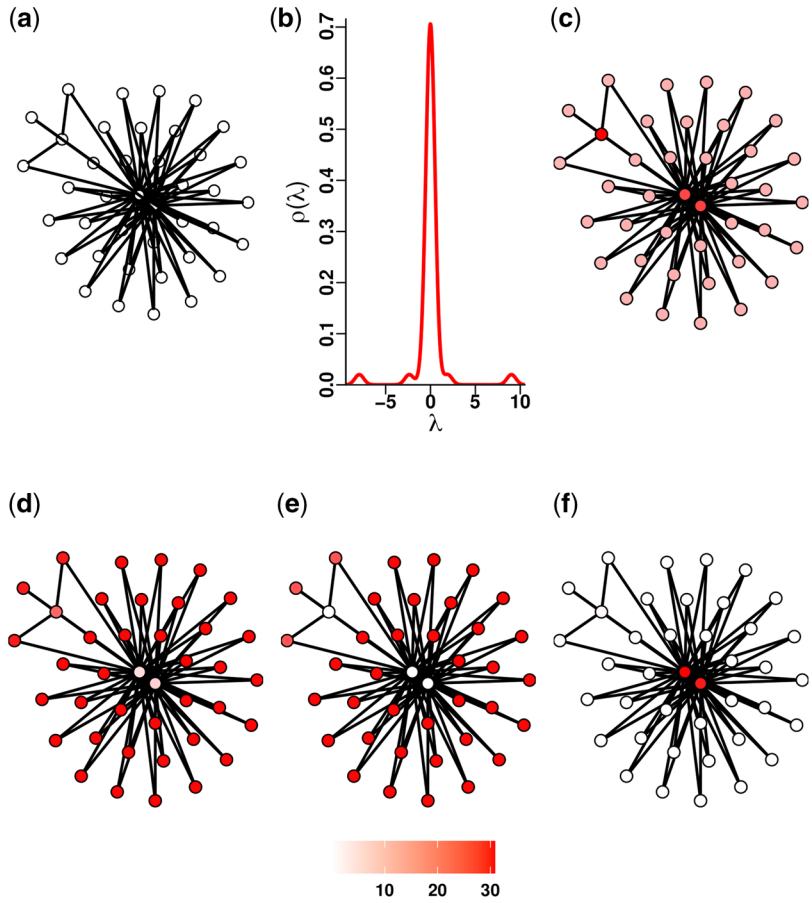

Figure 5. The darker red the vertex is, the higher its contribution to the considered eigenvalue. (a) Example of a graph generated with the Barabási-Albert model with a scaling parameter $\gamma = 3.0$ and mean degree $m = 2$. (b) The spectral density of the graph described in panel (a). (c) Vertices related to the eigenvalue –1 ($\rho_i(\lambda = -1)$). (d) Vertices related to the eigenvalue +1 ($\rho_i(\lambda = +1)$). (e) Vertices related to the eigenvalue 0 ($\rho_i(\lambda = 0)$). (f) Vertices related to the largest eigenvalue ($\rho_i(\lambda = \lambda_1)$). To obtain the contribution of each vertex to a particular eigenvalue, we used Equation (3.3) with $\varepsilon = 0.01$.
Alt text: Visualization of vertex contributions to specific eigenvalues in a Barabási-Albert graph with scaling parameter $\gamma = 3.0$ and mean degree m=2. Panel (a) displays the graph structure. Panel (b) shows the graph's spectral density. Panels (c-f) highlight vertex-wise contributions to the eigenvalues –1, +1, 0, and the largest eigenvalue ($\lambda 1$), respectively. Vertex color intensity (darker red) represents a higher contribution of that vertex to the corresponding eigenvalue.

Figure 7 shows the contribution of the vertices for a graph generated using the Erdős-Rényi [41] model with 40 vertices. We set the probability p of adding an edge between two vertices as 0.051. The reason is to produce graphs with an average degree of 2, i.e. the same as the graph generated using the Barabási-Albert model. The graph generated using the Erdös-Rényi model, with 40 vertices and $p = 0.051$, does not exhibit significant symmetric structures. Therefore, only a pair of vertices contributes to the presence of eigenvalues $\lambda = \pm 1$. Several leaf and isolated vertices also contribute to the eigenvalue $\lambda = 0$. We observe that the vertices with the highest degrees contribute more to the largest eigenvalue (λ_1).

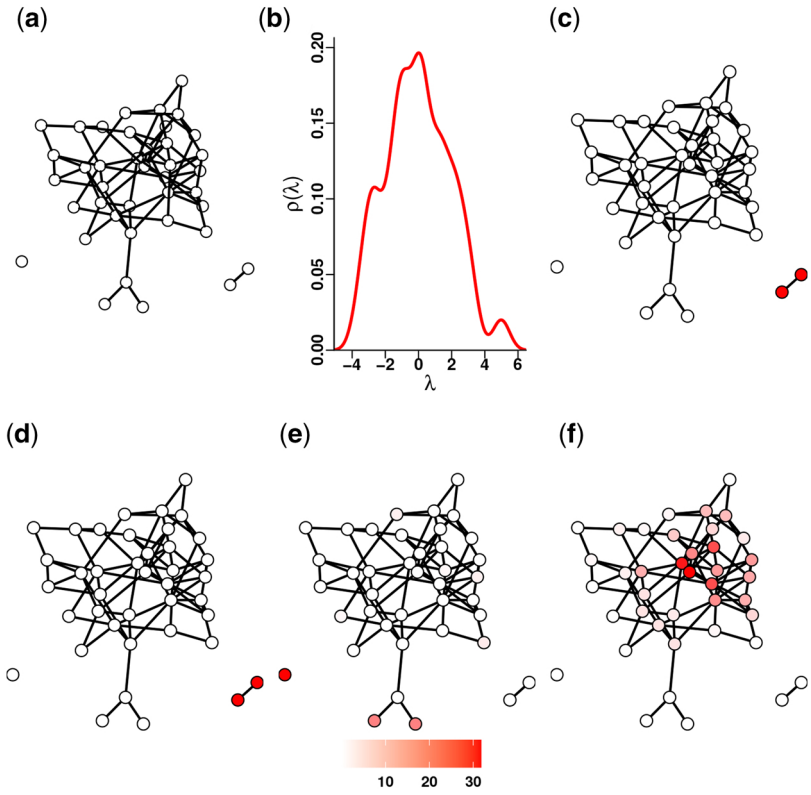

Figure 6. The darker red the vertex is, the higher its contribution to the considered eigenvalue. (a) Example of a graph generated with the Erdős-Rényi model with probability p of adding an edge between two vertices as 0.103. (b) The spectral density of the graph is described in panel (a). (c) Vertices related to the eigenvalue –1 ($\rho_i(\lambda = -1)$). (d) Vertices related to the eigenvalue +1 ($\rho_i(\lambda = +1)$). (e) Vertices related to the eigenvalue 0 ($\rho_i(\lambda = 0)$). (f) Vertices related to the largest eigenvalue ($\rho_i(\lambda = \lambda_1)$). To obtain the contribution of each vertex to a particular eigenvalue, we used Equation (3.3) with $\varepsilon = 0.01$. **Alt text:** Visualization of vertex contributions to specific eigenvalues in an Erdős-Rényi graph with edge probability p = 0.103. Panel (a) shows the graph structure. Panel (b) displays the graph's spectral density. Panels (c-f) illustrate vertex-wise contributions to the eigenvalues –1, +1, 0, and the largest eigenvalue ($\lambda 1$), respectively. Darker red coloring indicates a higher contribution of a vertex to the corresponding eigenvalue.

Henceforth, considering Equation (3.4), the vertex-wise spectral density of a graph depends on the eigenvector localization [34]. This means that the importance of a vertex for a given eigenvalue λ relies on the magnitude of the i-th element of all eigenvectors whose associated eigenvalue is λ.

To show that our proposed measure is distinct and captures information that classical centrality measures do not, we generated 100 graphs with 40 vertices using the following random graph models:

- Watts-Strogatz with parameters $\bar{d} = 4$ and $p_w = 0.0$.
- Watts-Strogatz with parameters $\bar{d} = 4$ and $p_w = 0.10$.
- Barabási-Albert with parameters $m = 2$ and $\gamma = 0.5$.
- Barabási-Albert with parameters $m = 2$ and $\gamma = 3.0$.
- Erdős-Rényi graph with parameters $p = 0.103$ (generating graphs with an expected average degree of 4).

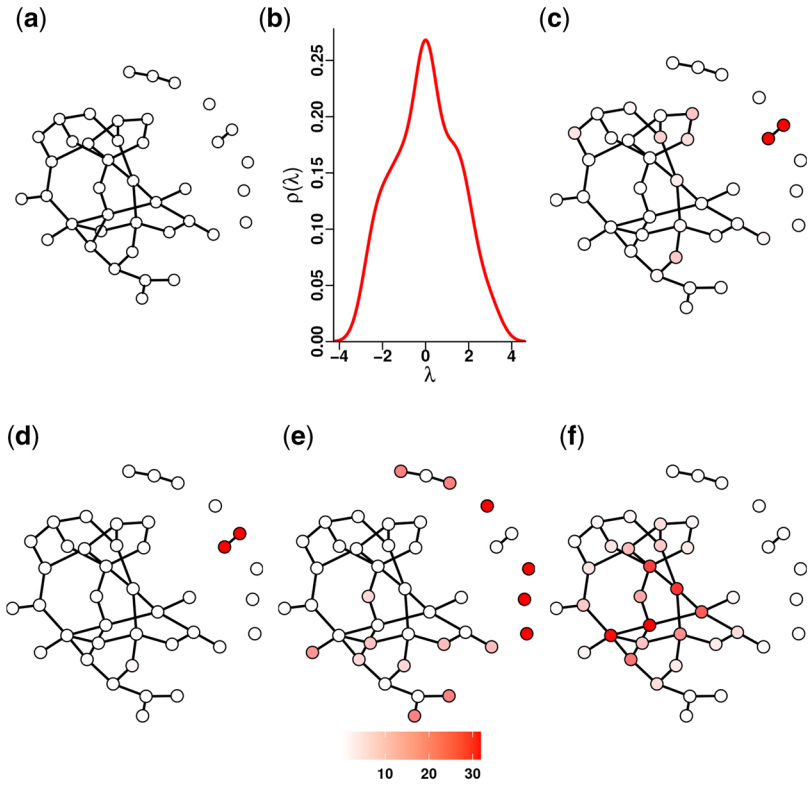

Figure 7. The darker red the vertex is, the higher its contribution to the considered eigenvalue. (a) Example of a graph generated with the Erdős-Rényi model with probability p of adding an edge between two vertices as 0.051. (b) The spectral density of the graph is described in panel (a). (c) Vertices related to the eigenvalue –1 ($\rho_i(\lambda = -1)$). (d) Vertices related to the eigenvalue +1 ($\rho_i(\lambda = +1)$). (e) Vertices related to the eigenvalue 0 ($\rho_i(\lambda = 0)$). (f) Vertices related to the largest eigenvalue ($\rho_i(\lambda = \lambda_1)$). To obtain the contribution of each vertex to a particular eigenvalue, we used Equation (3.3) with $\varepsilon = 0.01$. **Alt text:** Visualization of vertex contributions to specific eigenvalues in an Erdős-Rényi graph with edge probability p = 0.051. Panel (a) shows the graph structure. Panel (b) displays the graph's spectral density. Panels (c-f) illustrate vertex-wise contributions to the eigenvalues –1, +1, 0, and the largest eigenvalue ($\lambda 1$), respectively. Darker red coloring indicates a higher contribution of a vertex to the corresponding eigenvalue.

- Erdős-Rényi graph with parameters $p = 0.051$ (generating graphs with an expected average degree of 2).

For each graph, we computed the degree, eigenvector centrality, closeness centrality, betweenness centrality, and clustering coefficient [42], along with the vertex importance for the eigenvalues -1, 0, 1, and the largest eigenvalue (λ_1) using $\varepsilon = 0.01$. We then calculated the Spearman correlation between our proposal and these measures. Table 1 presents the mean Spearman correlation and its standard deviation across the 100 graphs.

The vertex contribution for the largest eigenvalue (λ_1) strongly correlates with most centrality measures, particularly eigenvector centrality. This high correlation is expected, as the contribution of a vertex to λ_1 incorporates the entries of its corresponding eigenvector, which, in turn, is closely related to the degree of each vertex [43]. Consequently, other centrality measures—except for the clustering coefficient—also show some correlation [44, 45].

Regarding the relationship between centrality measures and the vertex contributions to the eigenvalues -1, 0, and 1, we do not observe strong or consistent correlations as we do with λ_1.

Table 1. Mean and standard deviation of the Spearman correlation between a centrality measure and the vertex contribution for a particular eigenvalue.

	Measure	Eigenvalue (λ)			
		-1	0	1	λ_1
Watts-Strogatz $\bar{d} = 4, p_w = 0$	Degree	–	–	–	–
	Eigenvector	-0.01 ± 0.03	-0.02 ± 0.03	-0.02 ± 0.03	0.02 ± 0.09
	Closeness	–	–	–	–
	Betweenness	-0.11 ± 0.00	0.04 ± 0.00	-0.17 ± 0.00	0.77 ± 0.00
	Clustering	–	–	–	–
Watts-Strogatz $\bar{d} = 4, p_w = 0.10$	Degree	-0.09 ± 0.15	-0.11 ± 0.17	-0.09 ± 0.16	0.85 ± 0.06
	Eigenvector	-0.06 ± 0.15	-0.09 ± 0.18	-0.06 ± 0.19	1.00 ± 0.00
	Closeness	-0.23 ± 0.16	-0.13 ± 0.18	0.06 ± 0.18	0.66 ± 0.12
	Betweenness	-0.25 ± 0.15	-0.12 ± 0.17	0.07 ± 0.17	0.55 ± 0.13
	Clustering	0.35 ± 0.16	0.07 ± 0.17	-0.21 ± 0.18	-0.24 ± 0.21
Barabási-Albert $m = 2, \gamma = 0.5$	Degree	-0.29 ± 0.13	-0.56 ± 0.18	-0.28 ± 0.17	0.79 ± 0.06
	Eigenvector	-0.26 ± 0.13	-0.32 ± 0.17	-0.23 ± 0.16	1.00 ± 0.00
	Closeness	-0.28 ± 0.13	-0.35 ± 0.17	-0.24 ± 0.15	0.94 ± 0.03
	Betweenness	-0.29 ± 0.14	-0.52 ± 0.17	-0.25 ± 0.17	0.7 ± 0.08
	Clustering	-0.02 ± 0.16	-0.12 ± 0.14	-0.21 ± 0.17	0.54 ± 0.13
Barabási-Albert $m = 2, \gamma = 3.0$	Degree	0.24 ± 0.24	-0.55 ± 0.07	0.24 ± 0.28	0.46 ± 0.12
	Eigenvector	-0.13 ± 0.28	0.03 ± 0.15	-0.14 ± 0.24	0.59 ± 0.22
	Closeness	0.04 ± 0.33	-0.28 ± 0.23	0.06 ± 0.33	0.58 ± 0.18
	Betweenness	0.25 ± 0.25	-0.56 ± 0.10	0.26 ± 0.29	0.41 ± 0.17
	Clustering	-0.24 ± 0.27	0.53 ± 0.17	-0.26 ± 0.3	-0.38 ± 0.22
Erdős-Rényi $p = 0.103$	Degree	-0.19 ± 0.18	-0.43 ± 0.19	-0.21 ± 0.17	0.88 ± 0.05
	Eigenvector	-0.14 ± 0.19	-0.29 ± 0.18	-0.18 ± 0.17	1.00 ± 0.00
	Closeness	-0.17 ± 0.19	-0.33 ± 0.17	-0.17 ± 0.17	0.91 ± 0.07
	Betweenness	-0.19 ± 0.17	-0.46 ± 0.18	-0.19 ± 0.16	0.72 ± 0.10
	Clustering	0.06 ± 0.16	-0.13 ± 0.15	-0.17 ± 0.17	0.49 ± 0.16
Erdős-Rényi $p = 0.051$	Degree	0.18 ± 0.18	-0.71 ± 0.12	0.18 ± 0.17	0.83 ± 0.07
	Eigenvector	0.16 ± 0.22	-0.42 ± 0.16	0.17 ± 0.2	0.98 ± 0.12
	Closeness	0.29 ± 0.19	-0.53 ± 0.12	0.29 ± 0.21	0.67 ± 0.25
	Betweenness	0.05 ± 0.16	-0.6 ± 0.12	0.07 ± 0.15	0.73 ± 0.08
	Clustering	–	–	–	–

*-12pt
We considered 100 graphs generated using the Watts-Strogatz, Barabási-Albert, and Erdős-Rényi models with different parameters. We computed the degree, eigenvector, closeness, betweenness, and clustering centrality, along with the vertex contributions for the eigenvalues -1, 0, 1, and λ_1, using $\varepsilon = 0.01$. "–" indicates that the centrality measure and the vertex contribution for a particular eigenvalue are constants. Therefore, the Spearman correlation is not defined.

This is because contributions to non-dominant eigenvalues often capture more subtle structural properties than centrality-related aspects.

Finally, to study the effect of choosing the parameter ε, we consider a graph generated by the Watts-Strogatz model with an average degree of 4, a rewiring probability of 0.10, $\lambda = -1$, and $\varepsilon \in \{10^{-1}, 10^{-2}, 10^{-3}, 10^{-4}\}$. Since ε acts as a smoothing parameter [27] and Equation (2.5) relates the entries of the eigenvector to the importance of the vertex, we expect that as ε approaches 0, the importance of a vertex to a particular eigenvalue becomes the weighted sum of the entries of the eigenvector corresponding exclusively to $\lambda = -1$. For large ε, the contribution of a vertex to a particular eigenvalue also considers the eigenvector entries corresponding to eigenvalues close to $\lambda = -1$.

Figure 8 shows the effect of ε on vertex contribution. As ε decreases, fewer vertices exhibit a large contribution. This occurs because, for small values of ε, the weighted sum of the entries of the eigenvectors corresponding to the eigenvalue -1 carries more weight than the entries associated

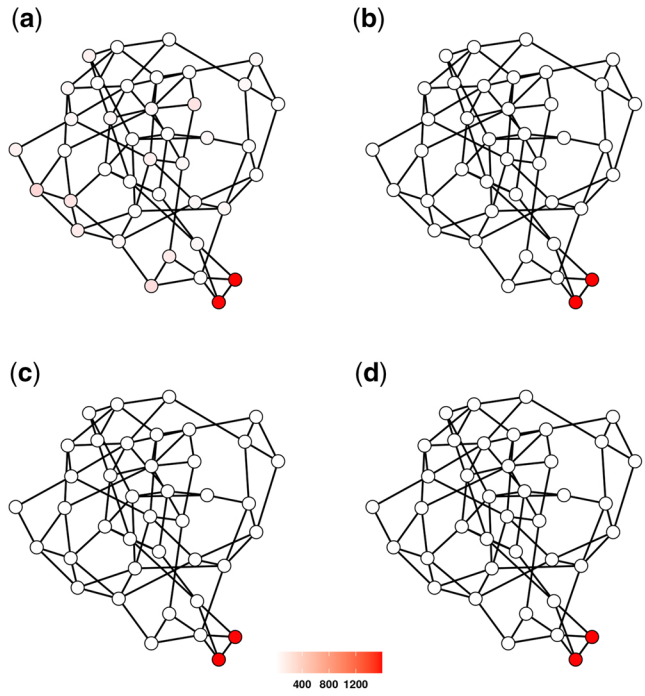

Figure 8. The darker red the vertex is, the higher its contribution to the eigenvalue -1 of a graph generated with the Watts-Strogatz model with a rewiring probability of 0.10 and mean degree 4. (a) Contribution of each vertex when $\varepsilon = 10^{-1}$. (b) Contribution of each vertex when $\varepsilon = 10^{-2}$. (c) Contribution of each vertex when $\varepsilon = 10^{-3}$. (d) Contribution of each vertex when $\varepsilon = 10^{-4}$.
Alt text: Four heatmaps showing vertex-wise contributions to the eigenvalue -1 in a graph generated by the Watts-Strogatz model with rewiring probability 0.10 and mean degree 4. Panels (a-d) show the contributions using different values of ε:10-1, 10-2, 10-3, and 10-4, respectively. Vertices are colored in shades of red, where darker red indicates a higher contribution to the eigenvalue. The progression across panels demonstrates how the resolution of the spectral decomposition changes with decreasing ε.

with other eigenvalues. Additionally, as ε decreases, the contribution of the vertices scales as $O(\varepsilon^{-1})$. Using $\varepsilon = 0.01$ already yields the same results as using smaller values.

4. APPLICATION

As a first application, we obtain the vertex-wise spectral density decomposition of two isospectral molecules [46]: 1,4-Divinylbenzene and 2-Phenylbutadiene. Since these molecules are isospectral with eigenvalues $\{-2.214, -1.675, -1.000, -1.000, -0.539, 0.539, 1.000, 1.000, 1.675, 2.214\}$, their spectral densities are equal. Figure 9 shows the graph representations of 1,4-Divinylbenzene and 2-Phenylbutadiene in panels (a) and (b), respectively. Notice that although they are isospectral, they are not isomorphic. Panels (c) and (d) display the vertex-wise decompositions of the graphs described in panels (a) and (b), respectively. Both molecules are composed only of carbon. Thus, we had to identify which atom of 1,4-Divinylbenzene corresponds to which atom of 2-Phenylbutadiene. To this end, we constructed a distance matrix among the vertex-wise densities of the two molecules. Then, we applied the Hungarian algorithm [47] to determine the assignment that minimizes the total L_2 distance.

Finally, panels (e) and (f) show the vertex-wise densities of the vertices with the smallest (vertex 2) and largest (vertex 9) L_2 distances, represented by solid and dotted lines, respectively. In panel (e), we observe only one line. This is because the L_2 distance between the vertex-wise densities of

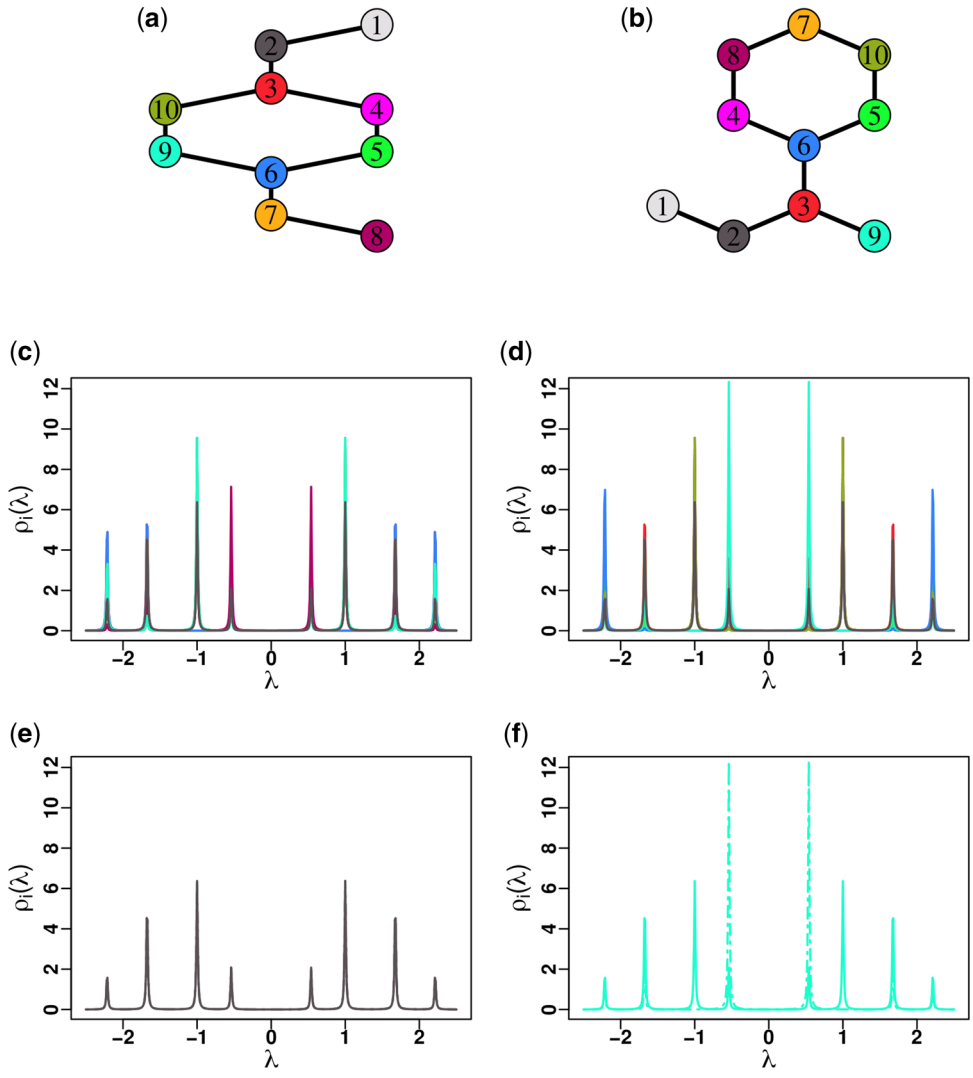

Figure 9. Graph representation of 1,4-Divinylbenzene (a) and 2-Phenylbutadiene (b), along with their respective vertex-wise decompositions in panels (c) and (d). We assigned the vertex labels using the Hungarian algorithm [47] to find the combination that minimizes the L_2 distance between the vertex-wise densities of the graph vertices. Finally, panels (e) and (f) show the vertex-wise densities of the vertices with the smallest (vertex 2) and the largest (vertex 9) L_2 distances, represented by solid and dotted lines, respectively. We observe that the vertex-wise densities of vertex 2 are equal, i.e. their L_2 distance is close to zero (panel (e)). This means that vertex 2 has a similar local neighborhood. On the other hand, the vertex-wise densities of vertex 9 are different (panel (f)). This means that vertex 9 has a very different local neighborhood. We set $\varepsilon = 0.01$ to obtain the vertex-wise decomposition.

Alt text: A figure comparing the graph structures and vertex-wise spectral decompositions of two chemical compounds: 1,4-Divinylbenzene (panel a) and 2-Phenylbutadiene (panel b). Panels (c) and (d) show each graph's vertex-wise spectral density decompositions, using vertex labels assigned by the Hungarian algorithm to minimize the L2 distance between corresponding vertices. Panels (e) and (f) display the spectral densities of the vertices with the smallest (vertex 2) and largest (vertex 9) L2 distances, represented by solid and dotted lines, respectively. Panel (e) shows nearly identical densities, indicating similar local neighborhoods, while panel (f) reveals distinct densities, reflecting structural differences. All decompositions were computed using ε =0.01.

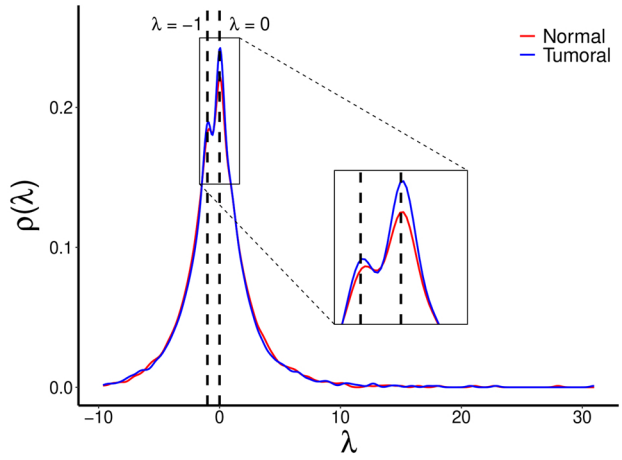

Figure 10. Spectral densities of the normal and tumoral gene networks. We can observe two peaks in spectral densities, one at -1 and another at 0 (dashed lines). Among them, the eigenvalue with the largest difference between normal and tumoral spectral densities is when $\lambda = 0$. We set $\varepsilon = 0.01$ to obtain the importance of each vertex.
Alt text: A line graph comparing the spectral densities of normal and tumoral gene networks. Two prominent peaks are visible near the eigenvalues -1 and 0, indicated by dashed vertical lines. The most significant difference between the two curves occurs at $\lambda = 0$, suggesting this eigenvalue is key in distinguishing the two networks. The spectral densities were computed using $\varepsilon = 0.01$.

vertex 2 in the graphs from panels (a) and (b) is close to zero (i.e. smaller than 10^{-10}), even though the overall structures of the graphs are different. This indicates that the weighted sum of their closed walks, where shorter walks have more significant weight (see Equation (2.6)), is equal, meaning that their local neighborhoods (considering vertices up to a distance of 2) are identical. In contrast, panel (f) displays a solid and a dotted line, indicating that these vertices have the most dissimilar local neighborhoods among the assignments.

As a second application, we consider the normal (1, 408 vertices and 6, 904 edges) and tumoral (1, 408 vertices and 7, 018 edges) breast gene interaction networks collected from [48] for illustration. We selected the largest connected component, which shared the same genes in both networks. Thus, we analyzed a normal network comprising 1, 319 vertices and 6, 904 edges and a tumoral network comprising 1, 319 and 6, 702 edges. We compared the two gene interaction networks using the semi-parametric analysis of graph variability (ANOGVA) test with 1000 bootstrap samples [17]. Briefly, the semi-parametric ANOGVA tests whether the estimated parameters of two or more random graph models are equal based on the graph's spectral densities. Following the literature, we considered that both networks were generated by a Barabási-Albert model [49, 50]. The semi-parametric ANOGVA test estimated as parameters 1.226 for the normal and 1.430 for the tumoral gene interaction networks, and a P value < 0.001. Therefore, we have statistical evidence that the estimated parameters are significantly different.

The next step in the analysis is identifying which genes or structures are different between the two gene interaction networks. To this end, we analyzed the graphs' spectral densities. Figure 10 shows the spectral densities of the normal and tumoral gene interaction networks. Visual inspection reveals that the differences between the spectral densities occur at eigenvalues -1 and 0. This finding aligns with previous works [25, 35, 36], which report that real-world networks exhibit degeneracies at these values. Then, we identified the genes related to these eigenvalues using the approach we proposed in Section 3 using Equation (3.3) with $\varepsilon = 0.01$ and $\lambda = -1, 0$.

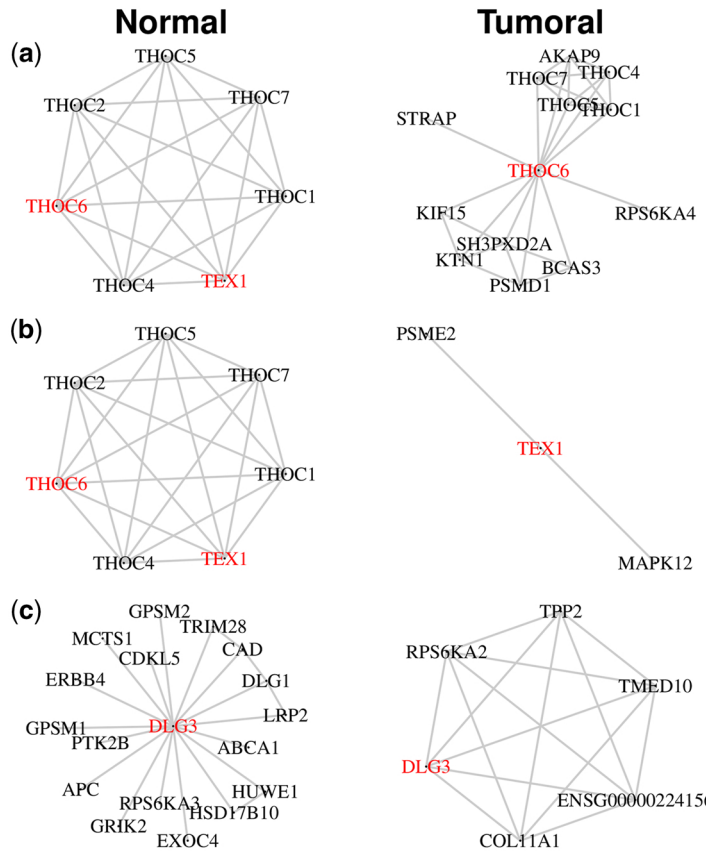

Figure 11. Egocentric networks of the three genes (red colored) with the largest difference in the vertex contribution for eigenvalue −1 between normal (left) and tumoral (right) gene interaction networks. Notice that the structure of egocentric networks changed considerably between conditions.
Alt text: Egocentric networks of the three genes (in red) with the largest difference in vertex contribution for eigenvalue -1 between normal (left) and tumoral (right) gene interaction networks. The structure of the egocentric networks changed considerably between conditions.

Figure 11 shows the three genes (and respective egocentric networks, i.e. the subnetwork comprising the referred gene and its direct neighbors) that most contribute to eigenvalue −1 differently between normal and tumoral gene interaction networks. Observe that the structure of egocentric networks centralized on genes THOC6, TEX1, and DLG3 differs between normal and tumoral conditions. THOC6 and TEX1 have the same neighborhood in the normal gene network. Also, their neighbors are fully connected. This means that THOC6 and TEX1 are symmetric vertices and are responsible for the −1 eigenvalue [26]. Since our proposed measure is associated with eigenvector localization, the genes with the highest importance may correspond to vertices where the eigenvectors related to the −1 entries are localized.

5. CONCLUSIONS

This work introduces the vertex-wise graph's spectral density decomposition, which measures the contribution of each vertex to a particular eigenvalue. We demonstrate the relationship between the vertex-wise spectral density, eigenvector localization, and the number of closed walks. We applied the vertex-wise graph's spectral density decomposition to identify atoms and genes with differential

connectivity in two conditions. We propose that analyzing vertex-wise spectral density enables us to uncover new structures in empirical graphs.

ACKNOWLEDGMENTS

Nothing to declare.

CONFLICT OF INTEREST

Nothing to declare.

FUNDING

This work has been supported by JSPS KAKENHI grant number JP25K15019, FAPESP grants 2013/07699-0, 2023/18337-3, 2024/03261-4, and 2024/09195-3, CNPq grants 306811/2022-7, 402309/2024-3, and 443972/2024-9, CAPES (finance code 001), Alexander von Humboldt Foundation, Wellcome Leap, and the MEXT Cooperative Research Project Program, Medical Research Center Initiative for High-Depth Omics and CURE: JPMXP1323015486 for MIB, Kyushu University.

DATA AVAILABILITY STATEMENT

No new data were generated or analysed in support of this research.

REFERENCES

1. Saade A, Krzakala F, Zdeborová L. Spectral clustering of graphs with the Bethe Hessian. *Adv Neural Inform Process Syst* 2014;**27**.
2. Ramos TC, Mourão-Miranda J, Fujita A. Spectral density-based clustering algorithms for complex networks. *Front Neurosci* 2023;**17**:926321.
3. Kruzick S, Moura JM. Graph signal processing: filter design and spectral statistics. In: *2017 IEEE 7th International Workshop on Computational Advances in Multi-Sensor Adaptive Processing (CAMSAP)*, p. 1–5. Curação: IEEE 2017.
4. Jin S, Zafarani R. The spectral zoo of networks: embedding and visualizing networks with spectral moments. In: *Proceedings of the 26th ACM SIGKDD International Conference on Knowledge Discovery & Data Mining*, p. 1426–34, 2020.
5. Sawlani S, Zhao L, Akoglu L. Fast attributed graph embedding via density of states. In: *2021 IEEE International Conference on Data Mining (ICDM)*, p. 559–68. Auckland: IEEE, 2021
6. Barnett GA, Jiang K, Hammond JR. Using coherencies to examine network evolution and co-evolution. *Soc Netw Anal Min* 2015;**5**:11.
7. Karalus S, Krug J. Reconstruction of evolved dynamic networks from degree correlations. *Phys Rev E* 2016;**93**:062306.
8. Pospelov N, Nechaev S, Anokhin K *et al* Spectral peculiarity and criticality of a human connectome. *Phys Life Rev* 2019;**31**:240–56.
9. Sato JR, Vidal MC, de Siqueira Santos S *et al* Complex network measures in autism spectrum disorders. *IEEE/ACM Trans Comput Biol Bioinform* 2015;**15**:581–7.
10. Fujita A, Vidal MC, Takahashi DY. A statistical method to distinguish functional brain networks. *Front Neurosci* 2017;**11**:66.
11. Wigner EP. On the distribution of the roots of certain symmetric matrices. *Ann Math* 1958;**67**:325–7.
12. Tran LV, Vu VH, Wang K. Sparse random graphs: Eigenvalues and eigenvectors. *Random Struct Algorithms* 2013;**42**:110–34.
13. Santos S.D.S, Fujita A, Matias C. Spectral density of random graphs: convergence properties and application in model fitting. *J Complex Netw* 2021;**9**:cnab041.
14. Takahashi DY, Sato JR, Ferreira CE *et al* Discriminating different classes of biological networks by analyzing the graphs spectra distribution. *PloS One* 2012;**7**:e49949.
15. Guzman GE, Takahashi DY, Fujita A. A fast parameter estimator for large complex networks. *J Complex Netw* 2022;**10**:cnac022.
16. De Domenico M, Biamonte J. Spectral entropies as information-theoretic tools for complex network comparison. *Phys Rev X* 2016;**6**:041062.

17. Fujita A, Silva Lira E, Siqueira Santos S. D *et al* A semi-parametric statistical test to compare complex networks. *J Complex Netw* 2020;**8**:cnz028.
18. Fujita A, Takahashi DY, Balardin JB *et al* Correlation between graphs with an application to brain network analysis. *Comput Stat Data Analysis* 2017;**109**:76–92.
19. Ribeiro AH, Vidal MC, Sato JR *et al* Granger causality among graphs and application to functional brain connectivity in autism spectrum disorder. *Entropy* 2021;**23**:1204.
20. Guzman GEC, Fujita A. Convolution-based linear discriminant analysis for functional data classification. *Information Sci* 2021;**581**:469–78.
21. MacArthur BD, Sánchez-García RJ. Spectral characteristics of network redundancy. *Phys Rev E Stat Nonlin Soft Matter Phys* 2009;**80**:026117.
22. Dorogovtsev SN, Goltsev AV, Mendes JF *et al* Spectra of complex networks. *Phys Rev E Stat Nonlin Soft Matter Phys* 2003;**68**:046109.
23. Golinelli O. Statistics of delta peaks in the spectral density of large random trees. arXiv, 2003, preprint cond-mat/0301437, preprint: not peer reviewed. DOI: 10.48550/arXiv.cond-mat/0301437.
24. Kamp C, Christensen K. Spectral analysis of protein-protein interactions in *Drosophila melanogaster*. *Phys Rev E Stat Nonlin Soft Matter Phys*2005;**71**:041911.
25. Yadav A, Jalan S. Origin and implications of zero degeneracy in networks spectra. *Chaos* 2015;**25**:043110.
26. Marrec L, Jalan S. Analysing degeneracies in networks spectra. *Epl* 2017;**117**:48001.
27. Newman M, Zhang X, Nadakuditi RR. Spectra of random networks with arbitrary degrees. *Phys Rev E* 2019;**99**:042309.
28. Newman M. Spectra of networks containing short loops. *Phys Rev E* 2019;**100**:012314.
29. Cantwell GT, Newman MEJ. Message passing on networks with loops. *Proc Natl Acad Sci U S A* 2019;**116**:23398–403.
30. Stöckmann H-J. Quantum chaos. *Quantum Chaos*, 2007.
31. Stein J, Stöckmann H-J. Experimental determination of billiard wave functions. *Phys Rev Lett* 1992;**68**:2867–70.
32. Biggs N, Biggs NL, Norman B. *Algebraic Graph Theory*. Cambridge University Press, 1993.
33. Albert R, Barabási A-L. Statistical mechanics of complex networks. *Rev Mod Phys* 2002;**74**:47–97.
34. Pastor-Satorras R, Castellano C. Distinct types of eigenvector localization in networks. *Sci Rep* 2016;**6**:18847.
35. Jalan S, Sarkar C, Madhusudanan A *et al* Uncovering randomness and success in society. *PLoS One* 2014;**9**:e88249.
36. Rai A, Pawar AK, Jalan S. Prognostic interaction patterns in diabetes mellitus II: a random-matrix-theory relation. *Phys Rev E Stat Nonlin Soft Matter Phys* 2015;**92**:022806.
37. Van Mieghem P. *Graph Spectra for Complex Networks*. Cambridge University Press, 2010.
38. Watts DJ, Strogatz SH. Collective dynamics of 'small-world' networks. *Nature* 1998;**393**:440–2.
39. Tian L, Liu C, Xie J. A partition method for graph isomorphism. *Phys Procedia* 2012;**25**:1761–8.
40. Burq N, Letrouit C. Delocalized eigenvectors of transitive graphs and beyond. arXiv, preprint arXiv:2407.12384, 2024, preprint: not peer reviewed. DOI: 10.48550/arXiv.2407.12384.
41. Erdos P, Rényi A *et al* On the evolution of random graphs. *Publ. Math. Inst. Hung. Acad. Sci* 1960;**5**:17–60.
42. Newman M. *Networks*. Oxford University Press; 2018.
43. Bolland JM. Sorting out centrality: an analysis of the performance of four centrality models in real and simulated networks. *Social Networks* 1988;**10**:233–53.
44. Lee C-Y. Correlations among centrality measures in complex networks. arXiv, https://doi.org/physics/0605220, 2006, preprint: not peer reviewed. DOI: 10.48550/arXiv.physics/0605220.
45. Batool K, Niazi MA. Towards a methodology for validation of centrality measures in complex networks. *PloS One* 2014;**9**:e90283.
46. Heilbronner E, Jones TB. Spectral differences between "isospectral" molecules. *J Am Chem Soc* 1978;**100**:6506–7.
47. Kuhn HW. The Hungarian method for the assignment problem. *Naval Research Logistics Quarterly* 1955;**2**:83–97.
48. Rai A, Pradhan P, Nagraj J *et al* Understanding cancer complexome using networks, spectral graph theory and multilayer framework. *Sci Rep* 2017;**7**:41676–16.
49. Bebek G. Identifying gene interaction networks. *Statistical Human Genetics: Methods and Protocols*, 2012;850:483–94.
50. Kikkawa A. Random matrix analysis for gene interaction networks in cancer cells. *Sci Rep* 2018;**8**:10607.